Regular Article

PHYSICAL CHEMISTRY RESEARCH
Published by the
Iranian Chemical Society
www.physchemres.org
info@physchemres.org

Phys. Chem. Res., Vol. 10, No. 1, 143-150, March 2022
DOI: 10.22036/pcr.2021.290926.1925

Graphene Oxide/Activated Clay/Gelatin Composites: Synthesis, Characterization and Properties

S. Merad Boudia, K.I. Benabadji* and B. Bouras

Laboratory of Organic Electrolytes and Polyelectrolytes Application (LAEPO). Department of Chemistry, Faculty of Sciences, Tlemcen University, B. P. 119 13000 Tlemcen, Algeria

(Received 17 June 2021, Accepted 24 September 2021)

In this work, graphene oxide/activated clay/Gelatin (GO/AC/G) composite blends were prepared by a simple solution mixing method. X-ray diffraction (XRD) and Fourier transform infrared (FTIR) spectroscopy were used to study the novelty in the structural characterization of the samples. The thermal stability of these materials was carried out using thermogravimetric analysis (TGA). The obtained results showed that a homogeneous mixture of AC, GO, and G was formed. XRD results indicated on successful formation of an intercalated structure in the composites. The disappearance of peaks at 2θ = 8.1° and 2θ = 13.5° were observed for montmorillonite and GO, respectively, indicating the homogenous distribution of the GO sheets into the activated clay structure. The interlayer spacing increased from 19.4 to 23.5 Å due to the insertion of gelatin molecules into the sheets of the clay. The IR spectrum of (GO/AC/G) composite revealed the presence of C-O-C bonds, C=C bending, C-OH vibration, and C=O bending. These results show that GO was composited with AC structure. Furthermore, an intense band of N-H of gelatin at 3419 cm^{-1} was ameliorated *via* the combination with absorption bonds of O-H, indicating the interaction of gelatin with the clay. A comparison of the thermograms of GO/AC and GO/AC/G showed that the thermal stability was improved in the new prepared composite. High adsorption potential and regeneration capability make the GO/AC and GO/AC/G composites the potential environmentally friendly materials for reducing dye pollution.

Keywords: Activated clay, Graphene oxide, Biopolymer, Gelatin, Composite

INTRODUCTION

Clay minerals have been used in the field of nanocomposites, especially to improve the polymer materials performance, due to their microscopic size and intercalation property. Clay minerals are economic sheet-like inorganic materials that have specific properties. Their crystal molecular structure is composed of one central alumina octahedral sheet and two silica tetrahedral sheets [1]. The atomic model of clay indicates that the hydroxyl groups on the surface of the aluminosilicates promote the formation of hydrogen bonding [2]. It is worth noting that the negative charge on clays provides a high adsorption capacity toward positively charged cations such as heavy metals, cationic dyes, *etc*. [3]. Materials with combined properties of two or more phases of natural origin seem to have alternative and innovative characteristics. In addition, a simple modification of clays using cationic polymers or surfactants can improve clays' capacities *via* simple ion-exchange reactions; the latter reactions cause several interactions between the cationic species and the adsorbate [3].

A large number of studies have explored to modify clay minerals: ion exchange with inorganic or organic cations, binding of inorganic and organic anions, grafting of organic compounds, pillaring by different types of poly (hydroxo metal) cations, reaction with acids, interlamellar, intraparticle, and interparticle polymerization, calcination and dehydroxylation, reaggregation and delamination of smectitic clay minerals, and physical treatments such as

*Corresponding author. E-mail: bismetdz@yahoo.fr

ultrasound, lyophilisation, and plasma [4].

A study showed that graphene oxide (GO) added an organic modification on the clay due to its hydrophilic and hydrophobic functional groups [5]. Graphene oxide (GO), as an important derivative of graphene, was easily obtained by extraction from animal tissue; GO has many oxygen-containing functional groups including C=O, -O-, -OH, and -COOH [5]. It is very available, inexpensive, and biodegradable. Also, GO has a strong affinity, large specific surface area, an excellent mechanical strength, and a high cation-exchange amount [6]. GO interacts with clay mineral particles *via* hydrogen bonding, electrostatic interaction, hydrophobic interaction, Lewis acid-base interactions, and so on, causing physical and chemical changes on properties of clay mineral. In addition, the O-functional groups of GO shows strong affinities for heavy metal ions, thus GO may have effect on the retention properties of clay mineral when they come in mutual contact [7] .

It's noted that there is a weak chemical reaction between graphene oxide and clay mineral due to electronegativity proprieties of the both species, so it's mandatory to add another component to facilitate their connection.

Biopolymers, such as gelatin, have received high interest since 2000s due to their wide range of applications. Gelatin (G) is a natural fibrous protein material, non-toxic, anti-carcinogenic, biocompatible, biodegradable, and it has a considerable number of active groups (amino, hydroxyl, and carboxyl). It is provided by partial hydrolysis of the triple helix structure of collagen, which can be easily obtained by extraction from animal tissue [8]. The incorporation of G can not only improve the ion-exchange behavior, but also ameliorate the properties such as swelling ability, mechanical and thermal stability [9].

Several recent studies have developed composites that combine two components such as GO and clay materials [5,10], GO and gelatin [11-12] and the other ones based on gelatin and bentonite beads [13]. To the best of our knowledge, the modification of activated clay using GO and gelatin has not been studied previously.

Considering the high performance and especial properties of G, GO, and AC, their combination may generate a novel material that holds promising potential for several applications such as water treatment. The main objective of this study is to explore the synergistic effect of AC, GO, and G components on the properties of the new prepared composite. The present work aims to explore the possibility of combining activated clay (AC), graphene oxide (GO), and hexadecyltrimethylammonium bromide (HDTMA-Br) as intercalation agent, and gelatin (G) in order to obtain GO/AC, GO/AC/HDTMA, and GO/AC/G materials. This new adsorbent material is intended for use in wastewater treatment to remove anionic and cationic dyes, heavy metal ions, and refractory organic contaminants.

EXPERIMENTAL

Materials

Graphite powder was provided by Sigma-Aldrich (99% purity) and used as received. Hexadecyltrimethylammonium bromide (HDTMABr) and gelatin were purchased from Sigma-Aldrich (99% purity) and used without further purification. Furthermore, sodium nitrate, sulphuric acid, potassium permanganate, and hydrogen peroxide were supplied by Sigma-Aldrich and used without further purification. All solutions were prepared using bidistilled water.

Clay activation (AC)

Activation of raw clay (RC) was carried out according to the method described in our earlier work [3]. Briefly, in order to remove impurities, such as carbonates, quartz, and organic matter, the clay was dispersed in bidistilled water, and the clay fraction (< 2 μm) was recovered through sedimentation. In order to obtain sodium bentonite, the solid phase was then saturated with sodium ions in a 1 M sodium chloride solution. This operation was repeated three times. When saturation was achieved, the resulting solid was washed with bidistilled water several times in order to remove excess salt; the final product was activated clay (AC). The hexamminecobalt(III) chloride was used to determine the cation exchange capacity (CEC), which was found equal to 85 meq g/100 g.

Synthesis of Graphene Oxide (GO)

Graphene oxide was synthesized from natural graphite powder by a modified Hummers method [14]. 1 g of graphite powder and 5 g of sodium nitrate were added into 23 ml concentrated sulfuric acid in an ice bath. After 20 min

stirring, 3 g of potassium permanganate was gradually added into the suspension while stirring as slowly as possible to prevent the temperature exceeding from 20 °C. After 45 min stirring, 45 ml of bidistilled water was slowly added into the mixture. The rapid increase in temperature caused by addition of water was controlled such that it remained less than 98 °C. After 1 h, the suspension was further diluted with 400 ml warm distilled water, after which 20 ml hydrogen peroxide (50%) was added to remove the residual potassium permanganate and manganese dioxide.

The graphene oxide was obtained through centrifugation of the suspension at 4000 rpm for 30 min. The supernatant was discarded, and the solid was washed three times with 100 ml of 5% hydrochloric acid solution. The same washing process was repeated using bidistilled water until the pH of the supernatant became neutral. The obtained product was dried at 80 °C for 24 h.

Synthesis of GO/AC/HDTMA composite

To obtain graphene oxide/activated clay (GO/AC) composite with a ratio (GO/AC) (w/w) of 10%, 500 mg of AC powder was mixed with a solution containing 50 mg of GO.

0.17 g of hexadecyltrimethylammonium bromide (HDTMA-Br) was separately dispersed in 20 ml of H_2O, and then added to the suspension of GO/AC10%, which was refluxed at 80 °C for 4 h to obtain (GO/AC/HDTMA) composite.

Afterwards, 60 mg of gelatin was added to the previous solution by continuously stirring for 120 min to obtain composite labelled (GO/AC/G). The suspension was centrifuged at 4000 rpm for 30 min. The supernatant was discarded, and the product was washed with bidistilled water for three times. Finally, the prepared composite was dried for 24 h at 80 °C.

Characterization

The XRD patterns of the samples were obtained with X-ray diffractometer ULTIMA IV (Rigaku, Tokyo, Japan), operating with Copper Kα radiation (λ = 1.54 Å) at 40 kV and 30 mA. All experiments were carried out at ambient temperature with 2θ varying between 2 and 40°, a scan speed of 2° min^{-1} and a step size of 0.02°.

Thermogravimetric analyses of the samples were obtained using High-resolution TGA (TA Instruments Q Series Q600 SDT). 10 mg of finely ground sample was heated in an open platinum crucible with a heating rate of 10 °C min^{-1} and temperature from 50 to 800 °C under a nitrogen atmosphere flow rate of 100 ml min^{-1}.

Infrared (IR) spectra of the samples were obtained using an Agilent Cary 600 Series FTIR Spectrometer equipped with DRIFT (Diffuse Reflectance Infra-red Fourier Transform) accessories. Spectra over the 4,000-400 cm^{-1} range were obtained by the co-addition of 64 scans with a resolution of 4 cm^{-1} and a mirror velocity of 0.6329 cm s^{-1}.

RESULTS AND DISCUSSION

X-ray Diffraction (DRX)

The XRD patterns of the samples are shown in Fig. 1. From the X-ray diffraction results, the major crystal phases contained in raw clay (RC) showed the presence of the peak relating to montmorillonite, in particular at d = 13.68 Å, 2θ = 6.45°. We noted the presence of quartz at d = 4.34 Å, 2θ = 20.40° and at d = 3.28 Å, 2θ = 27.08° as major impurity in RC.

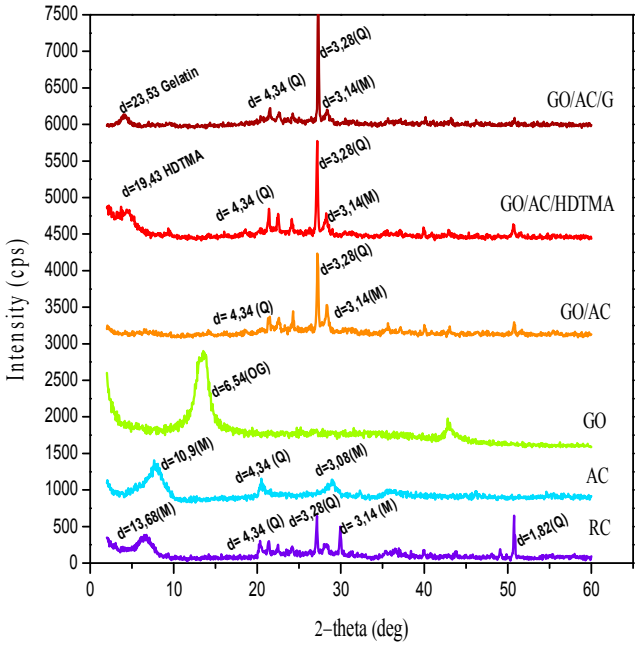

Fig. 1. XRD pattern of RC, AC, GO, GO/AC, GO/AC/HDTMA, GO/AC/G.

On the other hand, in the activated clay (AC) we noticed the shift of montmorillonite characteristic peak from 13.68 Å to 10.9 Å in AC diffractogram. This result suggests a parallel arrangement of the clay mineral layers.

In addition, successful oxidation of graphite to graphene was confirmed by X-ray diffraction (XRD). According to our results, after graphite oxidation, a sharp peak at $2\theta = 26.6°$ (d_{hkl} = 002, not shown) vanished and new peak appeared at 13.5° (d_{hkl} = 001). According to Bragg's equation [15], the calculated interlayer distance of graphene oxide was 6.55 Å. The increased d-spacing of GO compared to graphite (3.34 Å) resulted from the insertion of oxygen-functional groups and water molecules into graphene layers [16]. This result indicates that graphite was almost oxidized into GO [17].

No predominant GO peak was observed in GO/AC spectrum, indicating the homogenous distribution of GO on activated clay structure. The disappearance of montmorillonite peak at $2\theta = 8.1°$ indicates that the reactants on the GO/AC surfaces have been able to separate away the lamellae and produce a significantly less compact structure at very small angles. This phenomenon might indicate the possibility of the formation of an exfoliated structure in the final nanocomposite, as suggested by Ganjaee *et al*. [18]. The increased in the intensity of the observed peaks at $2\theta = 27.08°$ and 28.3° might be attributed to the change in the structure of activated clay [14].

The X-Ray diffraction patterns of modified clay GO/AC/HDTMA exhibited an interlayer spacing of 19.4 Å. This increase in the basal spacing for the modified clay demonstrates that at least a fraction of the cationic surfactant has replaced the hydrated interlayer cations [19].

When HDTMA molecules were introduced into the suspension of AC and GO, the crosslinking was formed in order to significantly increase the layer spacing of fabricated nanocomposite [5]. Indeed, XRD patterns of composites (GO/AC/G) changed distinctly compared to activated clay. The interlayer spacing increased from 19.4 to 23.5 Å due to the insertion of gelatin molecules into the sheets of GO/AC/HDTMA [20].

Thermal Analysis

In order to investigate the structural properties of GO, RC, AC, and the different composites, some thermogravimetric analysis (TGA) experiments were conducted under a nitrogen atmosphere.

The obtained results for TG (a) and DTG (b), presented in Fig. 2, indicate that unmodified activated clay (AC) the loss of the interlayer water. A second mass loss of 2.14% between 170 °C and 450 °C was related to the dehydroxylation of clay structure. The mass loss between 450 °C and 650 °C was attributed to dehydroxylation of the aluminosilicate groups in the clay structure [21].

For GO, the first stage, in the range of 50-160 °C, was attributed to the loss of adsorbed or hydrated water (about 11%). The significant weight loss (about 25%) occurred at the second stage in the range of 160-290 °C for GO, due to the release of steam, carbon monoxide, and carbon dioxide resulted from pyrolysis of the labile oxygen functional groups [22].

The same peaks of the activated clay were observed in GO/AC composite thermogram. Furthermore, a new extra weight loss of 6% between 200°C to 400°C might be due to the decomposition of GO in the impregnated catalyst. It has been shown that GO/AC has good thermal stability [23].

As shown in Fig. 2a, the weight losses of gelatin exhibited two decomposition stages. The first stage, in the exhibited a mass loss of 1.36% at 54 °C, corresponding to range of 40-200 °C, was attributed to the release of adsorbed or hydrated water (about 12%). The second stage, a weight loss of 55% observed between 200 and 470 °C, was related to the decomposition of amino acid fragments by an easy degradation [24].

As shown in Fig. 2, TG (a) and DTG (b) curves showed four decomposition stages for GO/AC/HDTMA sample.The first stage degradation at 50 °C was certainly attributed to adsorbed water.

The thermogram showed the presence of both surface bound and intercalated organic modifiers. By comparing TG curves of GO/AC/HDTMA and GO/AC samples, the resulting thermogram showed additional weight losses within the temperature range from 120 to 230 °C for the second degradation stage, and from 340 to 450 °C for the fourth one [25].

Since pure HDTMA bromide decomposes at about 250 °C [26], the peak observed between 120 and 230 °C corresponds to the decomposition of some cationic surfactant molecules adsorbed on the external surface of

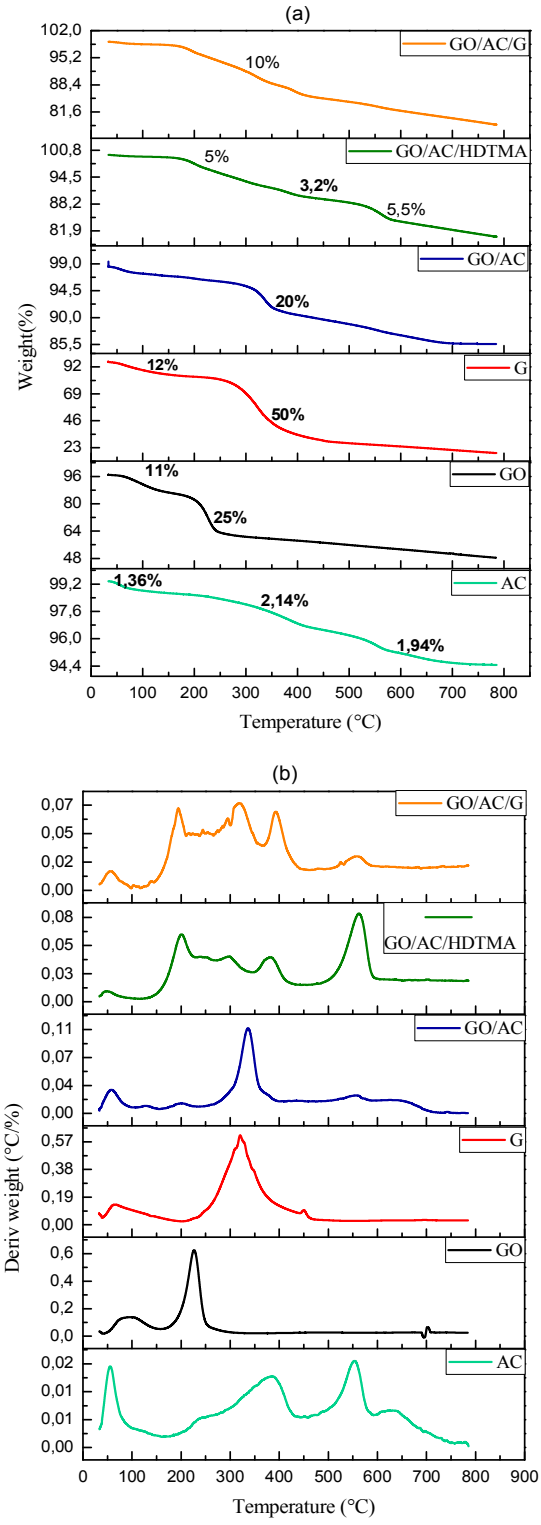

Fig. 2. TG (a) and DTG (b) analysis of different components AC, GO, G, GO/AC, GO/AC/HDTMA, GO/AC/G.

clay. The fourth most important weight loss occurred between 340 and 450 °C is certainly due to the decomposition of cationic surfactants intercalated within the AC layers [27]. The last weight loss occurred between 480 and 600 °C it related to the dehydroxylation of the aluminosilicates [28]. These findings indicate that the surfactant molecules adsorbed onto the external surface of the AC sample and intercalated in the interlayer spaces helped to improve the thermal stability of the corresponding composites [29].

TG and DTG curves of (GO/AC/G) composite showed a new weight loss at 323 °C. This peak is certainly related to the gelatin molecules. Comparing with TG and DTG curves of GO/AC/HDTMA sample, the thermograms showed the same weight losses for GO, AC, and HDTMA molecules.

Fourier Transform Infrared Spectroscopy

GO/AC/HDTMA, Gelatin, and GO/AC/G are shown in Figs. 3a and 3b. AC was characterized by the two broad bands at 3630 and 3440 cm^{-1}, which were attributed to the -OH stretching of the lattice hydroxyl and the -OH stretching of free H_2O, respectively. In addition, the Si-O stretching vibration band appeared at 1032 cm^{-1} and the O-H bending vibration band was observed at 1636 cm^{-1} [30].

Characteristic peaks observed at 1050, 1360, 1620, and 1713 cm^{-1} were ascribed to C-O-C bonds, C=C bending, C-OH vibration, and C=O bending, respectively, which are typical peaks of GO. These results suggest that graphite has been already oxidized to GO.

For GO/AC composite, all the peaks of GO and AC were appeared, and the bands of peaks belonging to GO became weak. These results illustrate that GO was composited with AC [31].

On the other hand, as shown in Fig. 3b in the FTIR spectrum of GO/AC/HDTMA, the new intense bands appeared at 2928 cm^{-1} and 2852 cm^{-1}, which characterized the presence of a symmetric ($\nu_s(CH_2)$) and an asymmetric ($\nu_{as}(CH_2)$) vibration of methylene groups on the carbon chain of surfactant [32]. Other vibration bands at 1386 cm^{-1} were arose of the C-H of methyl group in the ammonium groups.

In the case of the gelatin, new bands observed at 3419 cm^{-1} and at 1386 cm^{-1} were attributed to the N-H and

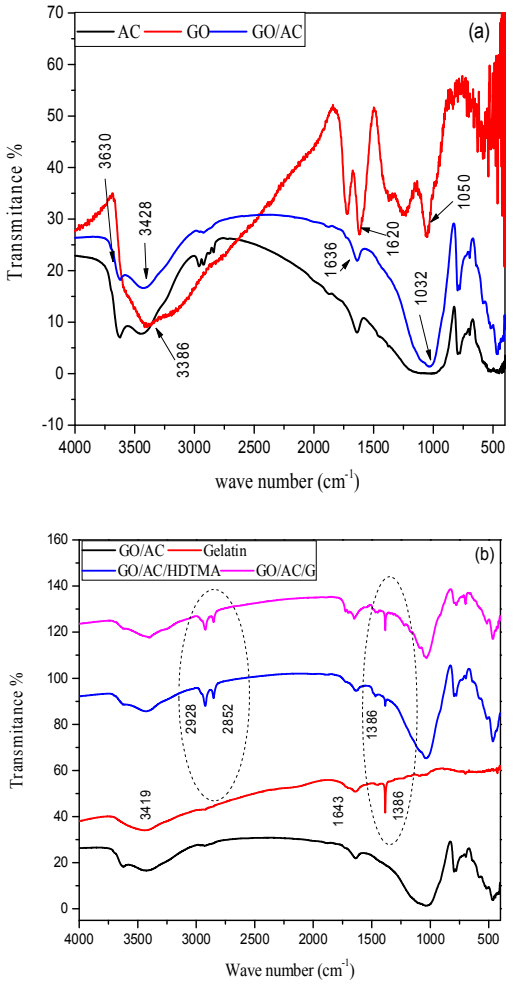

Fig. 3. FT -IR spectra (a) AC, GO, GO/AC 10%; (b) GO/AC, GO/AC/HDTMA, GO/AC/G, gelatin.

the C-H bonds, respectively. Another peak appeared at 1643 cm^{-1} was attributed to the stretching vibrations of the carbonyl group of amide [33].

The IR spectrum of GO/AC/G includes all the previous peaks, while the intensity of the band attributed to the N-H stretching vibration (3419 cm^{-1}) of gelatin, was improved by combination with absorption bonds of O-H, indicating the interaction between GO/AC/HDTMA and gelatin [34].

CONCLUSIONS

In this study, several composites such as GO/AC, GO/AC/HDTMA, and GO/AC/G were prepared by the modification of activated clay (AC) with an organic base graphene oxide (GO), a surfactant HDTMA, and gelatin biopolymer. The obtained composites were characterized by X-ray diffraction (XRD), infrared spectroscopy (FTIR), and thermal analysis (ATG/DTG).

The results from the FTIR spectroscopy suggested a good interaction between AC, GO, and G evidenced by the appearance of all characteristic peaks of AC, GO, and G in the final materials. The HDTMA was used as cross-linking agent. Moreover, XRD results showed that a partially exfoliated or intercalated structure was formed. The results of TGA analysis proved the thermal stability of the GO/AC/G composite.

Although several challenges need to be tackled, the current research progress suggests that these distinctive materials have a bright future in water purification. The applications of this composite in wastewater treatment to remove anionic and cationic dyes, heavy metal ions and organic contaminants are expected to be a great breakthrough in future.

REFERENCES

[1] Xu, W.; Chen, Y.; Zhang W.; Li, B., Fabrication of graphene oxide/bentonite composites with excellent adsorption performances for toluidine blue removal from aqueous solution. *Adv. Powder Technol.* **2019**, *30*, 493-501, DOI: 10.1016/j.apt.2018.11.028.

[2] Tao, E.; Ma, D.; Yang, S.; Hao, X., Graphene oxide-montmorillonite/sodium alginate aerogel beads for selective adsorption of methylene blue in wastewater. *J. Alloys Compd.* **2020**, *832*, 154833-154842, DOI: 10.1016/j.jallcom.2020.154833.

[3] Baouch, Z.; Benabadji, K. I.; Bouras, B., Adsorption of different dyes from aqueous solutions using organo-clay. *Phys. Chem. Res.* **2020**, *8*, 767-787, DOI: 10.22036/pcr.2020.234691.1787.

[4] Bergaya, F.; Lagaly, G., Surface modification of clay minerals. *Appl. Clay Sci.* **2001**, *19*, 1-3, DOI: 10.1016/S0169-1317(01)00063-1.

[5] Zhang, C.; Luan, J.; Chen, W.; Ke, X.; Zhang, H., Preparation of graphene oxide-montmorillonite nanocomposite and its application in multiple-

pollutants removal from aqueous solutions. *Water Sci. Technol.* **2019**, *79*, 323-333, DOI: 10.2166/wst.2019.046.

[6] Chang, Y. S., Adsorption of Cu(II) and Ni(II) ions from wastewater onto bentonite and bentonite/GO composite. *Environ. Sci. Pollut. Res.* **2020**, *27*, 33270-33296, DOI: 10.1007/s11356-020-09423-7.

[7] Wang, W.; Xu, H.; Ren, X.; Deng, L., Interfacial interaction of graphene oxide with Na-montmorillonite and its effect on the U(VI) retention properties of Na-montmorillonite. *J. Mol. Liq*. **2019**, *276*, 919-926, DOI: 10.1016/j.molliq.2018.12.130.

[8] Bociaga, D.; Bartniak, M.; Grabarczyk, J.; Przybyszewska, K., Sodium alginate/gelatine hydrogels for direct bioprinting-the effect of composition selection and applied solvents on the bioink properties. *Materials*. **2019**, *12*, 1-19, DOI: 10.3390/ma12172669.

[9] Fernandes, F. M.; Ruiz, A. I.; Darder, M.; Aranda, P.; Ruiz-Hitzky, E., Gelatin-clay bio-nanocomposites: Structural and functional properties as advanced materials. *J. Nanosci. Nanotechnol.* **2009**, *9* , 221-229, DOI: 10.1166/jnn.2009.J002.

[10] Yang, Y., Rapid adsorption of cationic dye-methylene blue on the modified montmorillonite/graphene oxide composites, *Appl. Clay Sci.* **2019**, *168*, 304-311, DOI: 10.1016/j.clay.2018.11.013.

[11] Panzavolta, S., Structural reinforcement and failure analysis in composite nanofibers of graphene oxide and gelatin, *Carbon N. Y.* **2014**, *78*, 566-577, DOI: 10.1016/j.carbon.2014.07.040.

[12] Zhan, J.; Morsi, Y.; Ei-Hamshary, H.; Al-Deyab, S. S.; Mo, X., Preparation and characterization of electrospun in-situ cross-linked gelatin-graphite oxide nanofibers. *J. Biomater. Sci. Polym. Ed.* **2016**, *27*, 385-402, DOI: 10.1080/09205063.2015.1133156.

[13] Li, W.; Ma, Q.; Bai, Y.; Xu, D.; Wu, M.; Ma, H., Facile fabrication of gelatin/bentonite composite beads for tunable removal of anionic and cationic dyes. *Chem. Eng. Res. Des.* **2018**, *134*, 336-346, DOI: 10.1016/j.cherd.2018.04.016.

[14] Ali, B.; Yusup, S.; Quitain, A. T.; Alnarabiji, M. S.; Kamil, R. N. M.; Kida, T., Synthesis of novel graphene oxide/bentonite bi-functional heterogeneous catalyst for one-pot esterification and transesterification reactions. *Energy Convers. Manag.* **2018**, *171*, 1801-1812, DOI: 10.1016/j.enconman.2018.06.082.

[15] Liu, B.; Wang, X.; Yang, B.; Sun, R., Rapid modification of montmorillonite with novel cationic Gemini surfactants and its adsorption for methyl orange. *Mater. Chem. Phys.* **2011**, *130*, 1220-1226, DOI: 10.1016/j.matchemphys.2011.08.064.

[16] Konicki, W.; Aleksandrzak, M.; Moszyński, D.; Mijowska, E., Adsorption of anionic azo-dyes from aqueous solutions onto graphene oxide: Equilibrium, kinetic and thermodynamic studies. *J. Colloid Interface Sci.* **2017**, *496*, 188-200, DOI: 10.1016/j.jcis.2017.02.031.

[17] Azarang, M.; Shuhaimi, A.; Sookhakian, M., Crystalline quality assessment, photocurrent response and optical properties of reduced graphene oxide uniformly decorated zinc oxide nanoparticles based on the graphene oxide concentration. *RSC Adv.* **2015**, *5*, 53117-53128, DOI: 10.1039/c5ra06123g.

[18] Ganjaee Sari, M.; Shamshiri, M.; Ramezanzadeh, B., Fabricating an epoxy composite coating with enhanced corrosion resistance through impregnation of functionalized graphene oxide-co-montmorillonite Nanoplatelet. *Corros. Sci.* **2017**, *129*, 38-53, DOI: 10.1016/j.corsci.2017.09.024.

[19] Naranjo, M.; Molina, J.; Sham, E. L.; Farfán Torres, E. M., Synthesis and characterization of HDTMA-organoclays: Insights into their structural properties. *Quim. Nova*. **2015**, *38*, 166-171, DOI: 10.5935/0100-4042.20140302.

[20] Zheng, J. P.; Li, P.; Ma, Y. L.; De Yao, K., Gelatin/montmorillonite hybrid nanocomposite. I. Preparation and properties. *J. Appl. Polym. Sci.* **2002**, *86*, 1189-1194, DOI: 10.1002/app.11062.

[21] Zhang, Z.; Luo, H.; Jiang, X.; Jiang, Z.; Yang, C., Synthesis of reduced graphene oxide-montmorillonite nanocomposite and its application in hexavalent chromium removal from aqueous solutions. *RSC Advances*. **2015**, *5*, 47408-47417, DOI: 10.1016/j.jhazmat.2019.06.016.

[22] Yang, Y.; Qi, M.; Xu, W.; He, S.; Men, Y., Natural polysaccharides-modified graphene oxide for adsorption of organic dyes from aqueous solutions. *J. Colloid Interface Sci.* **2017**, *486*, 84-96,

DOI: 10.1016/j.jcis.2016.09.058.

[23] Liu, H.; Xie, S.; Liao, J.; Yan, T.; Liu, Y.; Tang, X., Novel graphene oxide/bentonite composite for uranium(VI) adsorption from aqueous solution. *J. Radioanal. Nucl. Chem.* **2018**, *317*, 1349-1360, DOI: 10.1007/s10967-018-5992-0.

[24] De Figueredo, G. P., Synthesis of $MgAl_2O_4$ by gelatin method: Effect of temperature and time of calcination in crystalline structure. *Mater. Res.* **2017**, *20*, 254-259, DOI: 10.1590/1980-5373-MR-2017-0105.

[25] Sternik, D.; Gładysz-Płaska, A.; Grabias, E.; Majdan, M.; Knauer, W., A thermal, sorptive and spectral study of HDTMA-bentonite loaded with uranyl phosphate. *J. Therm. Anal. Calorim.* **2017**, *129*, 1277-1289, DOI: 10.1007/s10973-017-6384-3.

[26] Erdem, B.; Özcan, S.; Özcan, A., Preparation of HDTMA-bentonite: Characterization studies and its adsorption behavior toward dibenzofuran. *Surf. Interfa*ce *Anal.* **2010**, *42*, 1351-1356, DOI: 10.1002/sia.3230.

[27] Majdan, M.; Pikus, S.; Gajowiak, A.; Sternik, D.; Zieba, E., Uranium sorption on bentonite modified by octadecyltrimethylammonium bromide. *J. Hazard. Mater.* **2010**, *184*, 662-670, DOI: 10.1016/ j.jhazmat.2010.08.089.

[28] Xi, Y.; Mallavarapu, M.; Naidu, R., Preparation, characterization of surfactants modified clay minerals and nitrate adsorption. *Appl. Clay Sci.* **2010**, *48*, 92-96, DOI: 10.1016/j.clay.2009.11.047.

[29] Zhu, J.; Morgan, A. B.; Lamelas, F. J.; Wilkie, C. A., Fire properties of polystyrene-clay nanocomposites. *Chem. Mater.* **2001**, *13*, 3774-3780, DOI: 10.1021/cm000984r.

[30] Makhoukhi, B.; Djab, M.; Amine Didi, M., Adsorption of Telon dyes onto bis-imidazolium modified bentonite in aqueous solutions. *J. Environ. Chem. Eng.* **2015**, *3*, 1384-1392, DOI: 10.1016/j.jece.2014.12.012.

[31] Liu, L., Preparation of montmorillonite-pillared graphene oxide with increased single- and co-adsorption towards lead ions and methylene blue. *RSC Adv.* **2015**, *5*, 3965-3973, DOI: 10.1039/c4ra13008a.

[32] Houhoune, F.; Nibou, D.; Chegrouche, S.; Menacer, S., Behaviour of modified hexadecyltrimethylammonium bromide bentonite toward uranium species. *J. Environ. Chem. Eng.* **2016**, *4*, 3459-3467, DOI: 10.1016/j.jece.2016.07.018.

[33] Pilipenko, N., Tailoring swelling of alginate-gelatin hydrogel microspheres by crosslinking with calcium chloride combined with transglutaminase. *Carbohydr. Polym.* **2019**, *223*, 115035-115043, DOI: 10.1016/j.carbpol.2019.115035.

[34] Li, W.; Ma, Q.; Bai, Y.; Xu, D.; Wu, M.; Ma, H., Facile fabrication of gelatin/bentonite composite beads for tunable removal of anionic and cationic dyes. *Chem. Eng. Res. Des.* **2018**, *134*, 336-346, DOI: 10.1016/j.cherd.2018.04.016.